Bol. Soc. Paran. Mat.
©SPM – E-ISSN-2175-1188
SPM: www.spm.uem.br/bspm

(3s.) **v. 2026 (44) 4** : 1–16.
ISSN-0037-8712
doi:10.5269/bspm.80148

Hall Current and Heat Generation Impacts on Free Convective, Radiative, Chemically Reactive and Rotating Fluid Flow Over an Accelerated Isothermal Inclined Plate

Bettaiah Rangaswamy Srinivasa Prabhu [1,2], Joghyalla Santhosh Kumar* [1], Kammasandra Munivenkataswamy Praveena Kumara [1], Sibyala Vijaya Kumar Varma[1]

ABSTRACT: This work presents a comprehensive investigation of Magnetohydrodynamic (MHD) flow past an accelerated, isothermal, inclined plate within a rotating fluid environment, emphasizing the combined influence of Hall current and internal heat generation or absorption. The formulation incorporates variable mass diffusion, thermal radiation, and chemical reactions, leading to a coupled system of partial differential equations governing the velocity, temperature, and concentration fields. These equations are solved analytically using the Laplace transform technique under suitable initial and boundary conditions. The study distinguishes itself by systematically exploring how major physical parameters-such as the magnetic field, Hall current, rotational effects, porous medium permeability, radiation, and reactive species-shape the transport behaviour of the fluid. Validation against previously reported results confirms the accuracy and robustness of the model. Key findings reveal that fluid velocity increases with both the porous medium parameter(K)and the Hall current parameter, highlighting their role in enhancing flow acceleration. Temperature reduces noticeably with larger Prandtl numbers and heat absorption, while heat generation induces a marked rise in thermal distribution. These insights are relevant to several technological and natural processes, including MHD power systems, thermal management devices, and astrophysical fluid dynamics.

Key Words: Radiation, chemical reactions, rotation, Hall effects, Heat generation, absorption and MHD.

Contents

1. Introduction

The Hall current effect has a wide range of practical applications in various fields. Plasma physics is important for controlling and confining plasma in nuclear fusion reactors, as well as understanding space plasma dynamics such as solar winds and planetary magnetospheres. To convert the kinetic energy of fluids like plasma or liquid metal into electrical energy, magnetohydrodynamic (MHD) generators depend on Hall currents. Automotive systems and cell phones make use of Hall effect sensors, which sense magnetic fields primarily through Hall current effects. Furthermore, Hall effect thrusters use these currents for efficient ion propulsion in spacecraft. In astrophysics, Hall currents are critical for understanding cosmic plasma behaviour in phenomena such as accretion disks and interstellar matter interactions. For its important applications in heat transfer phenomena, many researchers have been studied different flow problems keeping in mind the hall current effect. Under the influence of H all effects and uniform suction or injection, Hazem and Ahmed [1] investigated the unstable MHD flow around a spinning disc. They found that after a certain distance, hall effects and higher injection parameter values make the fluid flow anticlockwise to the rotation of the disc. On the other hand, reduced values diminish the radial velocity component, encouraging the fluid to flow inward beyond the disc. Seth et al. [2] examined unstable

* Corresponding author.
2020 *Mathematics Subject Classification:* 76W05, 76R10, 76D05, 80A20, 35Q35, 76U05.
Submitted November 19, 2025. Published February 03, 2026

hydromagnetic free convection flow under the influence of Hall current and rotation. This process shows how heat and mass move through a thick, non-compressible, electrically conductive, chemically reactive, and optically thin fluid that radiates along an infinitely long plate. The plate moves abruptly within a porous material that sustains a consistently specified temperature and surface concentration. They found that Hall current tends to increase primary fluid velocity in areas that are close to the plate but has the opposite impact in areas that are away from it. Emad and Elsayed [3] proposed the heat and mass transfer characteristics along a vertical plate subjected to a Hall current and a uniform transverse magnetic field, taking into account the combined influence of buoyancy forces arising from both thermal and concentration gradients. Chi and Zhang [4]examined the impact of Hall effects on unstable fractional magnetohydrodynamic (MHD) free convection and heat transfer in a space environment, revealing that varying the fractional order produces effects opposite to those caused by changes in the Hall parameter, thereby enhancing both MHD flow and space heat transfer. Jiang et al. [5] employed a spectral collocation method combined with a second-order fractional backward difference scheme to study the effects of Hall currents on the unsteady MHD flow of a generalized second-grade fluid within a porous medium. Siddiqa and Hossain [6] investigated the effect of strong magnetic field and Hall current on the free convective boundary layer flow along a semi – infinite heated vertical surfaces Srinivasacharya and Kaladhar [7] investigated the flow of couple-stress electrically conducting fluid between two concentric cylinders, influenced by Hall and ion slip effects facilitated by a temperature-dependent heat source. Seth and Singh [8] investigated how Hall currents affect the flow characteristics of a thermally and electrically conducting viscous fluid in a rotating channel, leading to magnetically coupled convection. Paul et al. [9] investigated a mixed convective MHD heat-absorbing flow, incorporating Hall and viscous dissipation as parameters, which develops when a vertical porous plate is impulsively driven with a ramping surface temperature and concentration. Using the numerical Runge-Kutta-Fehlberg method, Isa et al. [10] studied the impacts of thermal radiation and Hall current on the magneto-natural convective flow of a dusty fluid. Important parameters appear to influence the fluid temperature; magnetic, radiation, and Hall parameters can cause it to increase, while the slip thermal parameter can cause it to decrease. Many other researchers have studied the hall effects [11,12,13,14,15]. Many industrial processes rely on the effects of heat sources and sinks on angled frameworks. These include fibre insulation for aircraft and spacecraft, microelectronic plate cooling, polymer compound synthesis, and aeronautical polymeric sheet processing. In industrial and engineering sciences, the heat source/sink effects enable numerous applications of combined heat and mass transfer. These include improved oil recovery, geothermal reservoirs, thermal insulation, cooling polymers, drying porous solids, nuclear reactors, oxidation, and synthesis materials. Dileep Kumar and Singh [16]employed a vertical concentric annular configuration to investigate the effects of heat sources, heat sinks, and induced magnetic fields on natural convection. Their findings indicate that introducing a heat sink leads to a decrease in temperature distribution, induced current density, induced magnetic field, and fluid velocity, whereas the presence of a heat source causes an enhance in all these parameters. Lavanya and Ratnam [17]have developed an analytical solution that takes into account radiation and mass transfer in the context of unsteady magnetohydrodynamic natural convection flow through a vertical porous plate in a porous medium. This flow occurs under a slip flow regime, incorporating a heat source/sink and the Soret effect. Hammad et al. [18] examined the influence of heat sources and sinks on the oscillations of thermal and concentration boundary layers across an inclined plate in a reduced gravitational field. They noted that an increase in the heat source parameter induces oscillations in heat transfer and enhances periodicity, while mass transfer improves with an increase in the heat sink parameter under reduced gravitational influence. Sankar Goud [19] explored MHD micropolar flow over a stretchable, porous surface, incorporating the effects of heat generation and variable suction/injection. According to their results a decline in the heat transfer coefficient with increased heat generation. Chamkha and Issa [20] analyzed magnetohydrodynamic (MHD) flow involving heat and mass transfer over a flat plate, accounting for heat generation or absorption and the thermophoretic effect. Their results demonstrated that increasing the strength of heat sources leads to a notable enhancement in the Stanton number. Mahdy [21] examined double-diffusive convection around a vertical cone within a porous medium, considering factors such as variable viscosity, chemical reactions, and heat generation. The study revealed that the Nusselt number decreases as the chemical reaction rate, Lewis number, or heat generation/absorption increases. Mabood et al. [22]investigated MHD flow with heat and mass transfer over a non-isothermal stretching sheet

using the Homotopy Analysis Method (HAM), incorporating effects of heat generation and transpiration. El-Amin [23]studied micropolar convection near a porous vertical surface subjected to internal heating and magnetic field influences. Miraj et al. [24,25]examined the combined influence of radiation and pressure work on convective flow around a sphere with internal heat generation. Their study showed that higher values of the heat generation parameter lead to increases in both velocity and temperature profiles. Hussain et al. [26] explored free convective heat transfer over an accelerating plate within a rotating system, incorporating Hall effects, heat absorption, and chemical reactions. They found that chemical reactions and rotational effects enhance the primary skin friction, whereas the Hall current, solutal buoyancy force, and medium permeability contribute to its reduction. In contrast, secondary skin friction rises with the presence of Hall current, rotation, solutal buoyancy force, and medium permeability but decreases when chemical reactions are considered. Dwivedi and Kumar Singh [27]discussed the impact of Hall currents on hydromagnetic convective flow occurring between two vertically aligned concentric cylinders, considering the effects of a heat source or sink. Their results indicated that the presence of a heat source enhances the heat transfer rate at the inner cylinder while reducing it at the outer cylinder, whereas the heat sink produces the reverse behavior. Recently, Ramaprasad et al. [28] investigated the impacts of radiation and chemical reaction on unsteady MHD flow over an accelerated isothermal inclined plate in a rotating fluid, considering variable mass diffusion. The present study focuses on an unsteady MHD flow over an accelerated isothermal inclined plate subjected to radiation and first-order chemical reactions in a rotating fluid. The unsteady nature of the flow is essential because many thermal and MHD systems experience time-dependent behaviour during start-up, acceleration, or transient heating conditions. The accelerated isothermal inclined plate models practical surfaces whose velocity varies with time while being maintained at a constant temperature, capturing realistic convection effects influenced by inclination and gravity. Although several related investigations exist, the combined influence of Hall current and heat generation or absorption in such a rotating, reactive, and diffusive environment has not been thoroughly explored. This study addresses this gap by analysing how Hall current, magnetic field, rotation, mass diffusion, thermal radiation, and heat generation/absorption modify velocity, temperature, and concentration distributions. Engineering applications—such as MHD generators, cooling and thermal management devices, and astrophysical plasma flows—require accurate understanding of these coupled effects. Numerical evaluations are carried out for a range of Grashof numbers, Hall parameters, heat generation/absorption rates, porous medium parameters, and Sherwood numbers. Results for the velocity, temperature, and concentration fields are presented, and the corresponding Nusselt and Sherwood numbers are computed for selected parameter combinations. The findings are validated by comparison with the results of [28], confirming the reliability of the developed model.

2. Mathematical Model of the Problem

The following assumptions are used to establish the governing equations:

- Pressure gradient force is neglected.
- An electric field and induced magnetic fields are neglected.
- Viscous dissipation, Darcy dissipation, joule dissipation effects are ignored.
- The flow is driven by buoyancy forces and also motion of the fluid.
- For the porous medium, Darcy brinkman model is considered.
- q_r is the radiative flux for an optimal thick fluid.
- First order chemical reaction is taken into consideration.
- Consider the flow, which rotates over an accelerated, isothermal inclined plate and is unsteady, free convective, radiative, and chemically reactive.
- The effects of Hall current and heat generation or absorption are incorporated.

- The fluid and plate continue to rotate as rigid bodies about the z-axis, with an angular velocity of $Omega$are assumed.
- B_0represents the strength of magnetic effects in the normal flow direction, as illustrated in Fig. 1
- Initially, the temperature and concentration are treated asT_{inf}andC_{inf}, respectively.
- When $t^* > 0$, the plate starts moving with a velocity of $u = u_0 t^*$ in its own plane.
- As the time progresses, the plate's temperature enhances to T_w and the concentration near the plate C_w also increases linearly. Since the plate extends infinitely along the plane $z = 0$, all physical parameters depend only on z^* and t^*.

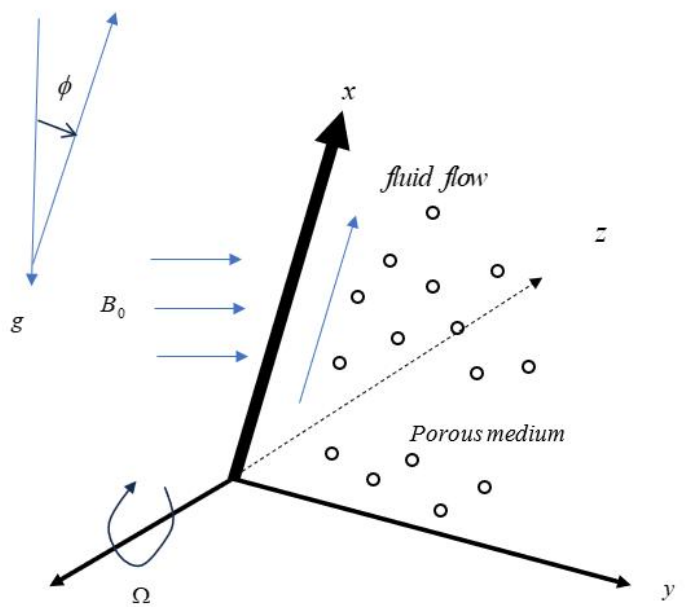

Figure 1: Schematic represent of the flow problem.

Equations that administered flow problem [22,23] are as follows: Momentum equations:

$$\frac{\partial u}{\partial t^*} - 2\Omega^* v^* = g\cos\phi\left\{\beta\cos\phi(T - T_\infty) + \beta^*(C^* - C^*_\infty)\right\} + \nu\frac{\partial^2 u}{\partial z^{*2}} - \frac{\sigma B_0^2(u + mv^*)}{\rho(1 + m^2)} - \frac{\nu}{K}u \tag{1}$$

$$\frac{\partial v^*}{\partial t^*} + 2\Omega^* u = \nu\frac{\partial^2 v^*}{\partial z^{*2}} - \frac{\sigma B_0^2(v^* - mu)}{\rho(1 + m^2)} - \frac{\nu}{K}v^* \tag{2}$$

Energy equation:

$$\rho C_p\frac{\partial T}{\partial t^*} = K\frac{\partial^2 T}{\partial z^{*2}} - \frac{\partial q_r}{\partial z^*} - Q_0(T - T_\infty) \tag{3}$$

Species diffusion equation:

$$\frac{\partial C^*}{\partial t^*} = D\frac{\partial^2 C}{\partial z^{*2}} - K_r^*(C^* - C^*_\infty) \tag{4}$$

Subject to the boundary conditions:

$$\begin{aligned}
&u(z,t)=0, \quad T(z,t)=T_\infty, \quad C^*(z,t)=C^*_\infty && \text{for } t^*\le 0\\
&u(z,t)=U_0^* f(t), \quad T(z,t)=T^*_w+(T^*_w-T^*_\infty)t^*, \quad C^*(z,t)=C^*_w+(C^*_w-C^*_\infty)t^* && \text{at } z=0\\
&u(z,t)\to 0, \quad T(z,t)\to T_\infty, \quad C^*(z,t)\to C^*_\infty && \text{as } z\to\infty
\end{aligned} \tag{5}$$

The non-dimensional parameters are given by the following expressions:

$$U=\frac{u}{(\nu u_0)^{1/3}}, \quad V=\frac{v^*}{(\nu u_0)^{1/3}}, \qquad t=t^*\left(\frac{u_0^2}{\nu}\right)^{1/3}, \qquad Z=z\left(\frac{u_0}{\nu^2}\right)^{1/3}, \qquad \theta=\frac{T-T_\infty}{T_w-T_\infty},$$

$$\mathrm{Pr}=\frac{\mu C_p}{K}, \qquad C=\frac{C^*-C^*_\infty}{C^*_w-C^*_\infty}, \quad \mathrm{Gr}=\frac{g\beta(T_w-T_\infty)}{u_0}, \quad \mathrm{Gm}=\frac{g\beta^*(C^*_w-C^*_\infty)}{u_0} \tag{6a}$$

$$\mathrm{Sc}=\frac{\nu}{D}, \qquad K_r^*=K_r^*\left(\frac{\nu}{u_0^2}\right)^{1/3}, \quad A=\left(\frac{u_0}{\nu}\right)^{1/3}, \qquad R=\frac{16a^*\sigma T_\infty^{4/3}}{Ku_0^{2/3}}, \quad \Omega^*=\Omega\left(\frac{u_0^2}{\nu}\right)^{1/3},$$

$$K_p=K\left(\frac{u_0}{\nu^2}\right)^{2/3}, \quad M=\frac{\sigma B_0^2\nu^{1/3}}{\rho u_0^{2/3}}, \qquad Q_H=\frac{Q_0}{\rho C_p}\left(\frac{\nu}{u_0^2}\right)^{1/3}, \quad \mathrm{Gr}'=\frac{g\beta(T_w-T_\infty)}{u_0} \tag{6b}$$

Using the above quantities, the leading equations given in eqns. (1) to (4) reduce to:

$$\frac{\partial U}{\partial t}-2\Omega V=\mathrm{Gr}'\cos\phi\,\theta+\mathrm{Gm}\cos\phi\,C+\frac{\partial^2 U}{\partial Z^2}-M\frac{(U+mV)}{(1+m^2)}-\frac{U}{K_p} \tag{7}$$

$$\frac{\partial V}{\partial t}+2\Omega V=\frac{\partial^2 V}{\partial Z^2}-M\left(\frac{V-mU}{1+m^2}\right)-\frac{V}{K_p} \tag{8}$$

$$\frac{\partial \theta}{\partial t}=\frac{1}{\mathrm{Pr}}\frac{\partial^2\theta}{\partial Z^2}-\left(\frac{R}{\mathrm{Pr}}+Q_H\right)\theta \tag{9}$$

$$\frac{\partial C}{\partial t}=\frac{1}{\mathrm{Sc}}\frac{\partial^2 C}{\partial Z^2}-K_r^*C \tag{10}$$

The corresponding boundary conditions are:

$$\begin{cases}
U(Z,t)=0,\ \theta(Z,t)=0,\ C(Z,t)=0, & \text{for } t\le 0,\\
U(Z,t)=t,\ \theta(Z,t)=1,\ C(Z,t)=t, & \text{at } Z=0,\ t>0,\\
U(Z,t)\to 0,\ \theta(Z,t)\to 0,\ C(Z,t)\to 0, & \text{as } Z\to\infty,\ t>0.
\end{cases} \tag{11}$$

The free convective flow of a radiative, chemically reactive fluid past an accelerating inclined plate is governed by the coupled partial differential equations (7) to (10), with the corresponding boundary conditions specified in equation (11). To address equations (7) and (8), a complex velocity is defined as

$$q(z,t)=u(z,t)+iv(z,t).$$

$$\frac{\partial q}{\partial t}=Gr\cos\phi\,\theta+Gm\cos\phi\,C+\frac{\partial^2 q}{\partial z^2}-\lambda q \tag{12}$$

Where,

$$\lambda=M\left(\frac{1-im}{1+m^2}\right)+\frac{1}{K_p}+2i\Omega \tag{13}$$

In terms of non-dimensional quantities, the associated initial and boundary conditions are as follows:

$$\begin{cases} q = 0,\ \theta = 0,\ C = 0, & \forall z,\ t \le 0, \\ q = t,\ \theta = 1,\ C = t, & \text{at } z = 0,\ t > 0, \\ q \to 0,\ \theta \to 0,\ C \to 0, & \text{as } z \to \infty,\ t > 0. \end{cases} \tag{14}$$

3. Laplace Transformation Method

Using the Laplace transformation approach, the non-dimensional governing equations (9), (10), and (11) are solved, subject to the associated initial and boundary conditions defined in equation (13). The expressions for $C(z,t)$, $\theta(z,t)$, and $q(z,t)$ are given by

$$\begin{aligned} C(z,t) = {} & \exp(-z\sqrt{Kr\,Sc})\left(\frac{t}{2} - \frac{z\sqrt{Sc}}{4\sqrt{Kr}}\right)\operatorname{erfc}\left(\frac{z\sqrt{Sc}}{2\sqrt{t}} - \sqrt{Kr\,t}\right) \\ & + \exp(z\sqrt{Kr\,Sc})\left(\frac{t}{2} + \frac{z\sqrt{Sc}}{4\sqrt{Kr}}\right)\operatorname{erfc}\left(\frac{z\sqrt{Sc}}{2\sqrt{t}} + \sqrt{Kr\,t}\right) \end{aligned} \tag{15}$$

$$\begin{aligned} \theta(z,t) = \frac{1}{2}\Bigg\{ & \exp\left(-z\sqrt{Pr}\right)\operatorname{erfc}\left(\frac{z\sqrt{Pr}}{2\sqrt{t}} - \sqrt{\frac{R}{Pr} + Q_H\,t}\right) \\ & + \exp\left(z\sqrt{Pr}\right)\operatorname{erfc}\left(\frac{z\sqrt{Pr}}{2\sqrt{t}} + \sqrt{\frac{R}{Pr} + Q_H\,t}\right)\Bigg\} \end{aligned} \tag{16}$$

$$q(z,t) = \chi_1 + \frac{Gr\cos\phi}{(\mathrm{Pr}-1)}\left(-\chi_2 + \chi_3 + \chi_4 - \chi_5\right) + \frac{Gm\cos\phi}{(\mathrm{Sc}-1)}\left(-\chi_6 - \chi_7 + \chi_8 + \chi_9 + \chi_{10} - \chi_{11}\right) \tag{17}$$

Where,

$$\chi_1 = \exp(-z\sqrt{\lambda})\left(\frac{t}{2} - \frac{z}{4\sqrt{\lambda}}\right)\operatorname{erfc}\left(\frac{z}{2\sqrt{t}} - \sqrt{\lambda t}\right) + \exp(z\sqrt{\lambda})\left(\frac{t}{2} + \frac{z}{4\sqrt{\lambda}}\right)\operatorname{erfc}\left(\frac{z}{2\sqrt{t}} + \sqrt{\lambda t}\right)$$

$$\chi_2 = \frac{1}{2a}\left[\exp(-z\sqrt{\lambda})\operatorname{erfc}\left(\frac{z}{2\sqrt{t}} - \sqrt{\lambda t}\right) + \exp(z\sqrt{\lambda})\operatorname{erfc}\left(\frac{z}{2\sqrt{t}} + \sqrt{\lambda t}\right)\right]$$

$$\chi_3 = \frac{e^{at}}{2a}\left[\exp(-z\sqrt{\lambda + a})\operatorname{erfc}\left(\frac{z}{2\sqrt{t}} - \sqrt{(\lambda + a)t}\right) + \exp(z\sqrt{\lambda + a})\operatorname{erfc}\left(\frac{z}{2\sqrt{t}} + \sqrt{(\lambda + a)t}\right)\right]$$

$$\chi_4 = \frac{1}{2a}\left[\exp\left(-z\sqrt{\frac{R}{Pr}}\right)\operatorname{erfc}\left(\frac{z\sqrt{Pr}}{2\sqrt{t}} - \sqrt{\frac{R}{Pr}t}\right) + \exp\left(z\sqrt{\frac{R}{Pr}}\right)\operatorname{erfc}\left(\frac{z\sqrt{Pr}}{2\sqrt{t}} + \sqrt{\frac{R}{Pr}t}\right)\right]$$

$$\chi_5 = \frac{e^{at}}{2a}\left[\exp\left(-z\sqrt{R + aPr}\right)\operatorname{erfc}\left(\frac{z}{2\sqrt{t}} - \sqrt{\frac{R}{Pr} + at}\right) + \exp\left(-z\sqrt{R + aPr}\right)\operatorname{erfc}\left(\frac{z}{2\sqrt{t}} + \sqrt{\frac{R}{Pr} + at}\right)\right]$$

$$\chi_6 = \frac{1}{2b^2}\left[\exp(-z\sqrt{\lambda})\operatorname{erfc}\left(\frac{z}{2\sqrt{t}} - \sqrt{\lambda t}\right) + \exp(-z\sqrt{\lambda})\operatorname{erfc}\left(\frac{z}{2\sqrt{t}} + \sqrt{\lambda t}\right)\right]$$

$$\chi_7 = \frac{A_1}{b}$$

$$\chi_8 = \frac{e^{at}}{2b^2}\left[\exp\left(-z\sqrt{\lambda+b}\right)\operatorname{erfc}\left(\frac{z}{2\sqrt{t}}-\sqrt{(\lambda+b)t}\right)+\exp\left(z\sqrt{\lambda+b}\right)\operatorname{erfc}\left(\frac{z}{2\sqrt{t}}+\sqrt{(\lambda+b)t}\right)\right]$$

$$\chi_9 = \frac{1}{2b^2}\left[\exp\left(-z\sqrt{Kr\,Sc}\right)\operatorname{erfc}\left(\frac{z\sqrt{Sc}}{2\sqrt{t}}-\sqrt{Kr\,t}\right)+\exp\left(z\sqrt{Kr\,Sc}\right)\operatorname{erfc}\left(\frac{z\sqrt{Sc}}{2\sqrt{t}}+\sqrt{Kr\,t}\right)\right]$$

$$\chi_{10} = \frac{1}{b}\left[\exp\left(-z\sqrt{Kr\,Sc}\right)\left(\frac{t}{2}-\frac{z\sqrt{Sc}}{4\sqrt{Kr}}\right)\operatorname{erfc}\left(\frac{z\sqrt{Sc}}{2\sqrt{t}}-\sqrt{Kr\,t}\right)\right.$$
$$\left.+\exp\left(z\sqrt{Kr\,Sc}\right)\left(\frac{t}{2}+\frac{z\sqrt{Sc}}{4\sqrt{Kr}}\right)\operatorname{erfc}\left(\frac{z\sqrt{Sc}}{2\sqrt{t}}+\sqrt{Kr\,t}\right)\right]$$

$$\chi_{11} = \frac{e^{bt}}{2b^2}\left[e^{-z\sqrt{(Kr+b)Sc}}\operatorname{erfc}\left(\frac{z\sqrt{Sc}}{2\sqrt{t}}-\sqrt{(Kr+b)t}\right)+e^{z\sqrt{(Kr+b)Sc}}\operatorname{erfc}\left(\frac{z\sqrt{Sc}}{2\sqrt{t}}+\sqrt{(Kr+b)t}\right)\right]$$

4. Important Quantities

The important quantities, the Nusselt number (Nu) and Sherwood number (Sh), are mathematically described in non-dimensional form as:

$$Nu = -\left(\frac{\partial\theta}{\partial z}\right)_{z=0} = \sqrt{(R+Q_H)\,Pr}\,\operatorname{erf}\left(\sqrt{\frac{R}{Pr}+Q_H\,t}\right)+\frac{\sqrt{Pr}}{\sqrt{\pi t}}\exp\left[-\left(\frac{R}{Pr}+Q_H\right)t\right]$$

$$\therefore \quad Sh = -\left(\frac{\partial C}{\partial z}\right)_{z=0} = \left(\frac{\sqrt{Sc}}{2\sqrt{Kr}}\right)\left[\operatorname{erf}\left(\sqrt{Krt}\right)+t\sqrt{KrSc}\,\operatorname{erf}\left(\sqrt{Krt}\right)+\frac{2}{\sqrt{\pi}}\left(\frac{\sqrt{Sc}}{\sqrt{t}}\right)\exp(-Krt)\right]$$

4. Result and Discussion

This study investigates the unsteady MHD-free convective, radiative, chemically reactive fluid flow over the accelerated isothermal insulated plate embedded porous medium with variable mass diffusion. The fluid is influenced by Hall current and heat generation and absorption. The next paragraph discusses the current parameters that have influenced the present investigation. Throughout our discussion of the results using a graphical view, we have consistently used fixed computational values for significant factors: For $Pr = 0.67$, $R = 1$, $Sc = 0.6$, $\phi = \pi/6$, $M = 2$, $Kr = 1$, $m = 1$, $\Omega = 0.5$, and $t = 0.2$. The influence of mass Grashof number G_m upon velocity profile has been depicted in Fig. 2.The mass Grashof number (G_m) significantly impacts the velocity profile through buoyancy forces. When $G_m > 0$, the plate cools, causing the fluid near it to become denser, which drives the flow upward and enhances the velocity profile. Conversely, when $G_m < 0$,,the heat from the plate causes the fluid around it to become less dense. As a result, buoyancy forces act downward, resisting fluid motion and causing the velocity profile to decrease and decay more rapidly. The Fig. 3 depicts the variation in velocity profile in response to a change in thermal Grashof number Gr. Positive Gr values indicate plate cooling, which leads to upward buoyancy forces and a higher velocity profile. As Gr increases, the buoyant forces become stronger, and the fluid rises more rapidly. In contrast, negative Grashof numbers signify heating, leading to downward buoyancy forces that produce a negative velocity profile. As Grbecomes more negative, the downward flow intensifies. The influence of the permeability parameter,K, on the thermal profile is depicted in Fig. 4. When the permeability of the porous medium is greater, it leads to a reduction in the velocity profile due to increased flow resistance. A higher porous medium parameter reflects a less permeable structure, which impedes the movement of the fluid and thus slows the flow. In Fig. 5, the effect of the Hall parameter, m, on the velocity profile (q) is shown. As the Hall parameter grows, so does the fluid's velocity, because the intensified magnetic field strengthens the Hall effect, with Lorentz forces acting on charged particles and boosting the voltage within the flow as velocity increases.

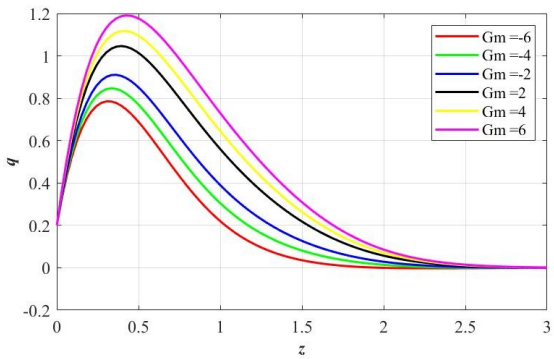

Figure 2: Impact of mass Grashof number G_m upon velocity profile $q(\xi)$.

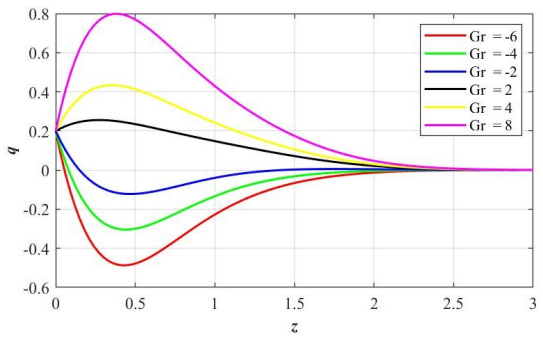

Figure 3: Impact of thermal Grashof number G_t upon velocity profile $q(\xi)$.

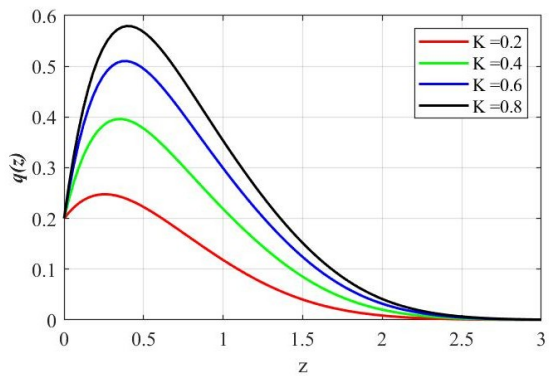

Figure 4: Impact of porosity parameter K upon velocity profile $q(\xi)$.

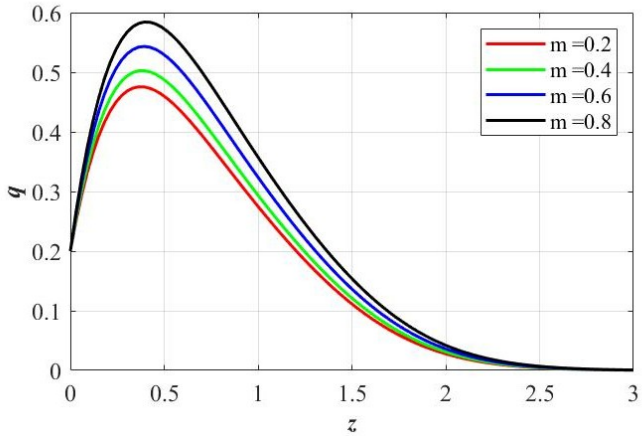

Figure 5: Impact of Hall parameter m upon velocity profile $q(\xi)$.

Fig. 6 illustrates the variation in temperature profile due to changes in Prandtl number for the given flow situation. As the Prandtl number(Pr) increases, the fluid become high viscous and hence leads to decrease the temperature. We observed a decrease in the temperature profile as the Prandtl number ($Pr = 0.7to10$)increased. Fig. 7 illustrates the influence of the heat generation or absorption parameterQ_H on temperature profiles. We observe that the presence of heat generation and absorption significantly influences the temperature profile. Here it is noticed that with increasing the heat generation, the thermal profile also increases due to additional thermal energy being added to the fluid, whereas a heat sink diminishes the fluid's temperature due to absorbing heat and cooling the fluid. Fig.8 explores the influence of the thermal radiation parameter(R) on the temperature distribution θ along the spatial direction z. As the value of increases, the temperature decreases more rapidly with distance from the boundary. This is due to the fact that higher thermal radiation enhances the energy loss from the system, allowing heat to dissipate more quickly. Consequently, greater radiative effects result in a steeper decline in temperature. This behavior highlights the significant role of radiation in accelerating heat transfer, especially in environments where radiative heat flux becomes dominant over conduction or convection.

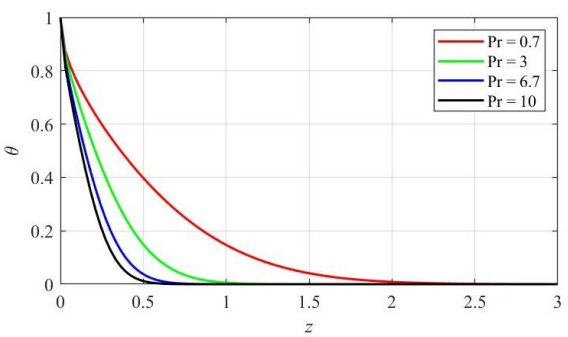

Figure 6: Impact of mass Prandtl number Pr upon temperature profile $q(\xi)$.

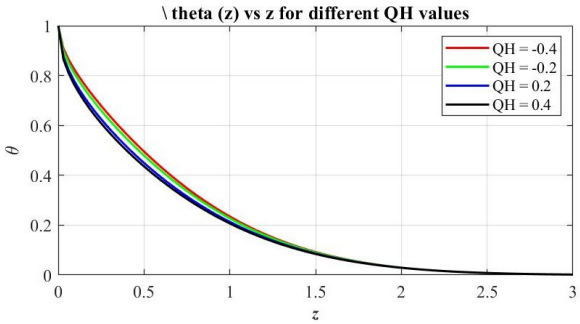

Figure 7: Impact of heat source/sink parameter Q_H upon temperature profile θ.

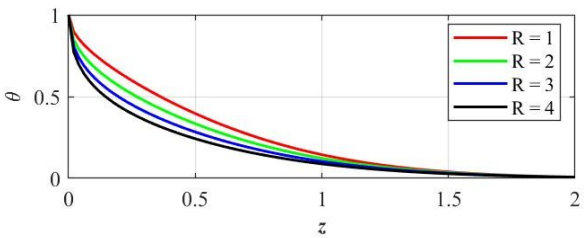

Figure 8: Impact of radiation parameter R upon temperature profile θ.

Fig. 9 depicts the influence of the Schmidt number Sc on the concentration distribution $C(z)$. An increase in Sc results in a steeper decline in concentration, reflecting a thinner concentration boundary layer.This behaviour arises because higher Sc corresponds to reduced mass diffusivity within the fluid. Consequently, species diffusion becomes weaker, causing concentration to diminish rapidly away from the wall. Fig. 10represents the variation of concentration subject to change in time. As time in progress, mass diffusion tends to spread the species throughout the fluid, which leads to gradual decrease the concentration of the fluid. It is observed that the wall concentration decreases with time.

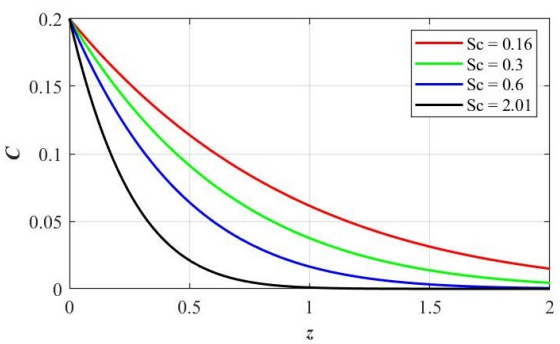

Figure 9: Impact of Schmidt number Sc upon concentration profile C.

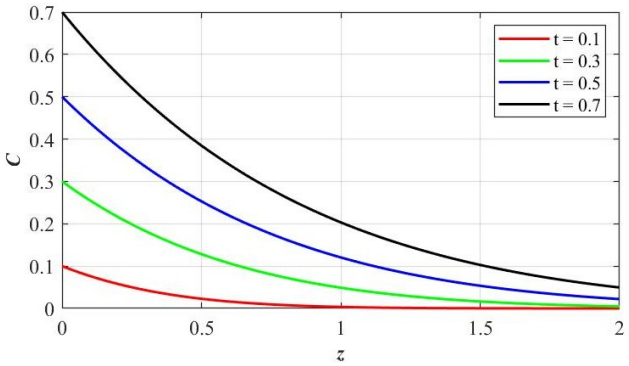

Figure 10: Impact of time t upon concentration profile C.

The 3D figures plotted to analyze the nature of heat and mass transfer for the parameters Q_H, R, K_r, and Sc are presented in Figs. 11 and 12. The Nusselt number increases with higher heat generation/absorption parameters and thermal radiation. A heat sink absorbs heat from the fluid, promoting effective cooling and reducing temperature gradients, which in turn enhances the Nusselt number. Likewise, stronger radiation further contributes to heat transport, leading to an additional rise in Nu. Increasing the values of K_r and Sc results in an increase in the Sherwood number (Sh), thereby improving mass transfer rates in the system. Figs. 13 and 14 provide a comparison of the present velocity and temperature profiles with those reported by Ramaprasad et al. [28].

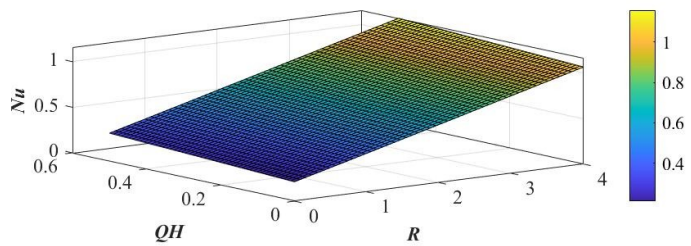

Figure 11: Variation of Nusselt number (Nu) against Q_H and R.

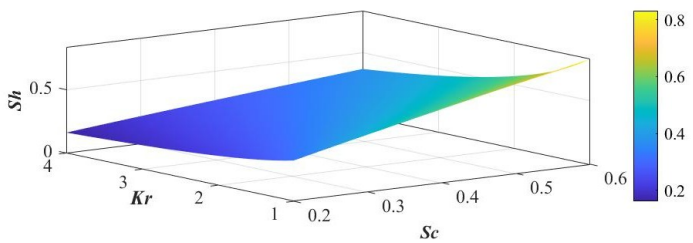

Figure 12: Variation of Sherwood number (Sh) against Kr and Sc.

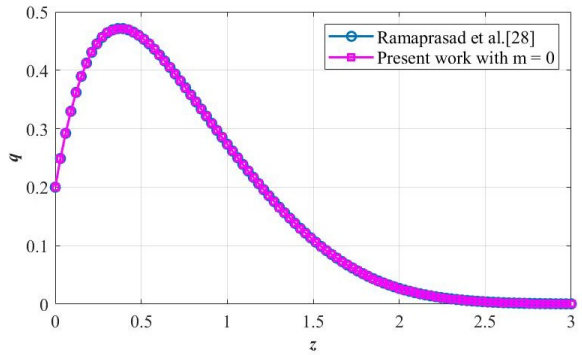

Figure 13: Comparison of velocity profiles with Ramprasad et al. [28]

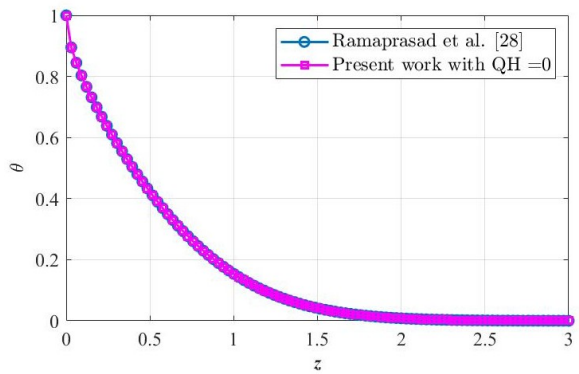

Figure 14: Comparison of temperature with Ramprasad et al. [28]

Table 1: **Nusselt number and Sherwood number for distinct (R, QH) and (Kr, Sc) respectively.**

R	QH	Nusselt Number	Kr	Sc	Sherwood Number
1	−0.2	0.38533	1	0.2	0.32178
	0.0	0.42329		0.4	0.58162
	0.2	0.46105		0.6	0.83126
2	−0.2	0.59920	2	0.2	0.23161
	0.0	0.63723		0.4	0.40497
	0.2	0.67512		0.6	0.56875
3	−0.2	0.81392	3	0.2	0.18829
	0.0	0.85174		0.4	0.32163
	0.2	0.88943		0.6	0.44593

In the absence of the Hall effect, heat generation, and absorption, our results for both velocity and temperature profiles overlap with those obtained by Ramprasad. Further, Table 1 shows the computa-

tional values of Nusselt number $(Nu)$and Sherwood number(Sh)

for both $R - Q_H$ and $Kr - Sc$ cases in the presence of distinct dimensionless constraints. The tabulated outcome shows that as Q_H increases from -0.2 to 0.2, the Nusselt number rises, showing more efficient heat dissipation. Also, Sh increases with increasing values of Kr and Sc due to enhanced mass transfer rates. Higher Kr and Sc values lead to faster species diffusion, improving mass transfer across the boundary layer.

5. Conclusion

This study examines the influence of Hall currents along with heat generation and absorption on free convection, radiation, and chemically reactive flow through a porous medium over an inclined plate in a rotating fluid environment. The key findings are summarized as follows.

- Increasing values of Gm and Gr, where both are positive, lead to enhancing the velocity profile.
- Reduced values of Gm and Gr, where both are negative, result in enhanced velocity profiles.
- The velocity profile enhances with higher effects of K and m.
- The temperature profile declines with increasing Prandtl numbers and heat absorption parameters, whereas it increases in the presence of heat generation.
- Increasing the thermal radiation R and Q_H enhances the heat transfer rate. In general, the radiation parameter and heat generation augment the thermal conductivity; as a sequence, the heat transfer advances.
- For increasing the chemical reaction Kr and Sc, the concentration rate enhanced. In general, the chemical reaction augments species diffusion; as a sequence, the mass diffusion improves.
- The findings of this study have implications in a wide range of applications, from astrophysics and fusion reactors to spacecraft and industrial processes.

Acknowledgments

The authors would like to thank the referees for their valuable comments and suggestions, which helped improve the quality and clarity of this paper.

References

1. A. A. Hazem, L. A. H. Ahmed, *Effects of Hall current on the unsteady MHD flow due to a rotating disk with uniform suction or injection*, Appl. Math. Model., **25** (2001) 1089–1098. https://doi.org/10.1016/S0307-904X(01)00033-6.
2. G. S. Seth, S. M. Hussain, S. Sarkar, *Effects of Hall current and rotation on MHD natural convection flow with heat and mass transfer past an impulsively moving vertical plate in the presence of radiation and chemical reaction*, Bulg. Chem. Commun., **46**(4) (2014) 704–718. https://doi.org/10.1016/j.asej.2013.09.014.
3. M. A. Emad, M. E. E. Elsayed, *Hall current effect on magnetohydrodynamic free-convection flow past a semi-infinite vertical plate with mass transfer*, Int. J. Eng. Sci., **39**(14) (2001) 1641–1652. https://doi.org/10.1016/S0020-7225(01)00020-9.
4. X. Chi, H. Zhang, *Numerical study for the unsteady space fractional magnetohydrodynamic free convective flow and heat transfer with Hall effects*, Appl. Math. Lett., **120** (2021) 107312. https://doi.org/10.1016/j.aml.2021.107312.
5. X. Jiang, Z. Hui, S. Wang, *Unsteady magnetohydrodynamic flow of generalized second grade fluid through porous medium with Hall effects on heat and mass transfer*, Phys. Fluids, **32**(11) (2020). https://doi.org/10.1063/5.0032821.
6. S. Siddiqa, M. A. Hossain, R. S. R. Gorla, *Hall current effects on magnetohydrodynamic natural convection flow with strong cross magnetic field*, Int. J. Therm. Sci., **71** (2013) 196–204. https://doi.org/10.1016/j.ijthermalsci.2013.04.016.
7. D. Srinivasacharya, K. Kaladhar, *Analytical solution of MHD free convective flow of couple stress fluid in an annulus with Hall and Ion-slip effects*, Nonlinear Anal. Model. Control, **16** (2011) 477–487. DOI:10.15388/NA.16.4.14090.
8. G. S. Seth, J. K. Singh, *Mixed convection hydromagnetic flow in a rotating channel with Hall and wall conductance effect*, Appl. Math. Model., **40** (2016) 2783–2803. https://doi.org/10.1016/j.apm.2015.10.015.
9. M. M. Paul, B. Prabhakar Reddy, J. M. Sunzu, *Hall and viscous dissipation effects on mixed convective MHD heat absorbing flow due to an impulsively moving vertical porous plate with ramped surface temperature and concentration*, Z. Angew. Math. Mech., (2024). https://doi.org/10.1002/zamm.202300210.

10. M. S. Isa, R. Mahat, N. M. Katbar, B. S. Goud, I. Ullah, W. Jamshed, S. M. Hussain, *Thermal radiative and Hall current effects on magneto-natural convective flow of dusty fluid: Numerical Runge–Kutta–Fehlberg technique*, Numer. Heat Transf. Part B: Fundam., (2024) 1–23. https://doi.org/10.1080/10407790.2024.2318452.

11. M. S. Ahmed, M. A. El-Aziz, *Effect of Hall currents and chemical reaction on hydromagnetic flow of a stretching vertical surface with internal heat generation/absorption*, Appl. Math. Model., **32**(7) (2008) 1236–1254. DOI:10.1016/j.apm.2007.03.008.

12. O. T. Bafakeeh, K. Raghunath, F. Ali, M. Khalid, E. S. M. Tag-ElDin, M. Oreijah, K. Guedri, N. B. Khedher, M. I. Khan, *Hall Current and Soret Effects on unsteady MHD Rotating Flow of Second-Grade Fluid through Porous Media under the Influences of Thermal Radiation and Chemical Reactions*, Catalysts, **12**(10) (2022). https://doi.org/10.3390/catal12101233.

13. K. Vafai, A. A. Khan, S. Sajjad, R. Ellahi, *The Study of Peristaltic Motion of Third Grade Fluid under the Effects of Hall Current and Heat Transfer*, Z. Naturforsch., **70**(4) (2015) 281–293. https://doi.org/10.1515/zna-2014-0330.

14. T. Hayat, A. Bibi, H. Yasmin, B. Ahmad, *Simultaneous effects of Hall current and homogeneous/heterogeneous reactions on peristalsis*, J. Taiwan Inst. Chem. Eng., **58** (2015) 28–38. https://doi.org/10.1016/j.jtice.2015.05.037.

15. M. Veera Krishna, N. Ameer Ahamad, A. F. Aljohani, *Thermal radiation, chemical reaction, Hall and ion slip effects on MHD oscillatory rotating flow of micro-polar liquid*, Alex. Eng. J., **60**(3) (2021) 3467–3484. https://doi.org/10.1016/j.aej.2021.02.013.

16. D. Kumar, A. K. Singh, *Effects of heat source/sink and induced magnetic field on natural convective flow in vertical concentric annuli*, Alex. Eng. J., **55**(4) (2016) 3125–3133. https://doi.org/10.1016/j.aej.2016.08.019.

17. B. Lavanya, A. L. Ratnam, *Radiation and mass transfer effects on unsteady MHD natural convective flow past a vertical porous plate embedded in a porous medium in a slip flow regime with heat source/sink and Soret effect*, Int. J. Eng. Tech. Res., **2** (2014).

18. A. S. Hammad, U. Zia, I. Asifa, S. A. Musaad, E. T. Alkathiri, M. E. El-Sayed, M. N. Murshed, A. M. Hassan, *Heat source/sink impact on wave oscillations of thermal and concentration boundary layer along inclined plate under lower gravitational region*, Case Stud. Therm. Eng., **53** (2024) 1–15. https://doi.org/10.1016/j.csite.2023.103829.

19. B. Shankar Goud, *Heat generation/absorption influence on steady stretched permeable surface on MHD flow of a micropolar fluid through a porous medium in the presence of variable suction/injection*, Int. J. Thermofluids, **7–8** (2020) 100044. https://doi.org/10.1016/j.ijft.2020.100044.

20. A. J. Chamkha, C. Issa, *Effects of heat generation/absorption and thermophoresis on hydromagnetic flow with heat and mass transfer over a flat surface*, Int. J. Numer. Methods Heat Fluid Flow, **10**(4) (2000) 432–449. https://doi.org/10.1108/09615530010327404.

21. A. Mahdy, *Effect of chemical reaction and heat generation or absorption on double-diffusive convection from a vertical truncated cone in porous media with variable viscosity*, Int. Commun. Heat Mass Transf., **37** (2010) 548–554. https://doi.org/10.1016/j.icheatmasstransfer.2010.01.007.

22. F. Mabood, W. A. Khan, A. I. M. Ismail, *Approximate analytical modelling of heat and mass transfer in hydromagnetic flow over a non-isothermal stretched surface with heat generation/absorption and transpiration*, J. Taiwan Inst. Chem. Eng., **54** (2015) 11–19. https://doi.org/10.1016/j.jtice.2015.03.022.

23. M. F. El-Amin, *Combined effect of internal heat generation and magnetic field on free convection and mass transfer flow in a micropolar fluid with constant suction*, J. Magn. Magn. Mater., **270**(1–2) (2004) 130–135. https://doi.org/10.1016/j.jmmm.2003.08.011.

24. M. Miraj, M. A. Alim, L. S. Andallah, *Effects of pressure work and radiation on natural convection flow around a sphere with heat generation*, Int. Commun. Heat Mass Transf., **38** (2011) 911–916. https://doi.org/10.1016/j.icheatmasstransfer.2011.04.019.

25. M. Miraj, M. A. Alim, M. A. H. Mamun, *Effect of radiation on natural convection flow on a sphere in presence of heat generation*, Int. Commun. Heat Mass Transf., **37** (2010) 660–665.

26. S. M. Hussain, J. Jain, G. S. Seth, M. M. Rashidi, *Free convective heat transfer with Hall effects, heat absorption and chemical reaction over an accelerated moving plate in a rotating system*, J. Magn. Magn. Mater., **422** (2017) 112–123. https://doi.org/10.1016/j.jmmm.2016.08.081.

27. N. Dwivedi, A. Kumar Singh, *Influence of Hall current on hydromagnetic natural convective flow between two vertical concentric cylinders in presence of heat source/sink*, Heat Transfer-Asian Res., (2020). https://doi.org/10.1002/htj.21669.

28. J. L. Ramaprasad, K. S. Balamurugan, L. Nageswara Rao, R. Swetha, *Radiative and chemical reaction effects on MHD flow past an accelerated isothermal inclined plate in a rotating fluid with variable mass diffusion*, Int. J. Chem. Sep. Technol., **3**(1) (2017) 1–13. https://doi.org/10.37628/jcst.v3i1.275.

Nomenclature:

A	constant
B_0	strength of the magnetic field (T)
C	Non-dimensional concentration
C^*	species concentration in the fluid (kg/m^3)
C_p	specific heat at a constant pressure (J/(kg·K))
C_w^*	wall concentration (kg/m^3)
D	mass diffusion coefficient (m^2/s)
erf	Error function
erfc	Complementary error function
g	acceleration due to gravity (m/s^2)
G_t	thermal Grashof number
G_m	mass Grashof number
K^*	permeability of the porous medium (m^2)
K	Porosity parameter
Kr	chemical reaction parameter
Nu	Nusselt number
m	Hall parameter
QH	Heat generation or absorption parameter (W/m^3)
R	thermal radiation number
t^*	Time (s)
Sc	Schmidt number
Sh	Sherwood number
u_0	velocity of plate (m/s)
x	spatial coordinate along the plate (m)
z	coordinate axis normal to the plate (m)

Greek symbols

k	Thermal conductivity (W/(m·K))
σ	Electrical conductivity (S/m)
ϕ	Inclined parameter (degree)
θ	Dimensionless fluid temperature
β	Coefficient of volume expansion of heat transfer (1/K)
β^*	Coefficient of volume expansion of mass transfer (1/K)
Ω	Rotation parameter
μ	Viscosity of fluid (Pa·s)
ν	Kinematic viscosity (m^2/s)
ρ	Density of the fluid (kg/m^3)

[1] *Department of Mathematics,*
School of Applied Sciences, REVA University,

India.

and

[2] *Department of Mathematics,*
Government first grade college, Kunigal, Karnataka, India.
India.
E-mail address: santoshkumarj@reva.edu.in